SUPPORTING INFORMATION (SI)

High-Efficiency All-Polymer Solar Cells with Poly-Small-Molecule Acceptors Having π-Extended Units with Broad Near-IR Absorption

*Ning Su,[a,b#] Ruijie Ma,[c#] Guoping Li,[b] Tao Liu,[c,] *Liang-Wen Feng,[b] Chenjian Lin,[b] Jianhua Chen,[b,*] Jun Song,[a,*] Yiqun Xiao,[d] Junle Qu,[a] Xinhui Lu,[d] Vinod K. Sangwan,[e,*] Mark C. Hersam,[b,e,f,*] He Yan,[c,*] Antonio Facchetti[b,g,*], Tobin J. Marks[b,*]*

[a] Center for Biomedical Optics and Photonics (CBOP) & College of Physics and Optoelectronic Engineering, Key Laboratory of Optoelectronic Devices and Systems, Shenzhen University, Shenzhen 518060, P. R. China

[b] Department of Chemistry, Center for Light Energy-Activated Redox Processes, and the Materials Research Center, Northwestern University, 2145 Sheridan Road, Evanston, Illinois 60208 (USA)

[c] Department of Chemistry and Hong Kong Branch of Chinese National Engineering Research Center for Tissue Restoration & Reconstruction, Hong Kong University of Science and Technology, Clear Water Bay, Kowloon, Hong Kong, China.

[d] Department of Physics, Chinese University of Hong Kong, New Territories, Hong Kong, China

[e] Department of Materials Science and Engineering, Northwestern University, Evanston, Illinois 60208 (USA)

[f] Department of Electrical and Computer Engineering, Northwestern University, Evanston, Illinois 60208 (USA)

[g] Flexterra Corporation, 8025 Lamon Avenue, Skokie, Illinois 60077 (USA)

[#] These authors contributed equally.

*To whom correspondence may be addressed. Email:

J. S. (songjun@szu.edu.cn),

T. L. (liutaozhx@ust.hk),

J. C. (jianhua.chen@northwestern.edu)

V. K. S. (vinod.sangwan@northwestern.edu)

M. C. H. (m-hersam@northwestern.edu)

H. Y. (hyan@ust.hk)

A. F. (a-facchetti@northwestern.edu)

T. J. M. (t-marks@northwestern.edu)

Table of Contents:

1. Materials and Methods

NMR spectra were recorded on a Bruker Avance III HD 500MHz system equipped with a TXO Prodigy probe. Chemical shifts for ^{1}H and ^{13}C spectra are referenced to residual protio-solvent signals (δ ^{1}H = 7.26 for $CDCl_3$, δ ^{13}C = 77.16 for $CDCl_3$) and chemical shifts are reported in ppm. Polymer molecular weights were measured on a Polymer Laboratories PL-GPC 220 instrument at 150 ºC calibrated with polystyrene standards and using trichlorobenzene as eluent. UV-Vis absorption spectra were recorded on a Varian Cary 100 UV-vis spectrophotometer. MS was performed on a Bruker AmaZon-SL instrument with ESI ionization in both negative and positive ionization mode. Elemental analyses (EA) of product polymers were carried out at Midwest Microlabs Inc. All reactions were carried out under an N_2 atmosphere, and all starting materials and solvents were purchased from commercial suppliers and used without further purification. PBDB-T and PM6 were purchased from Derthon Optoelectronic Materials ScienceTechnology Co. LTD, and BDT-Sn and BDTF-Sn were obtained from Flexterra Corporation; the starting material compound 2 was purchased from Aldrich.

2. Materials Synthesis

Compound 2 was obtained according to the reported reference.[1]

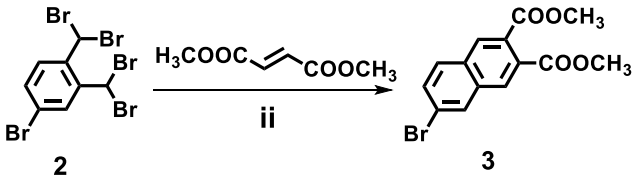

2 3

Synthesis of compound 3.

In a dry three-necked 500 mL flask, compound 2 (34.23 g, 68.51 mmol) and potassium iodide (18.08 g, 109.60 mmol) were combined and the mixture purged with N_2 followed by the addition of dry DMF (150 mL). The solution was heated to 80 ^{0}C and stirred for 30 min, next, dimethyl fumarate (11.84 g, 82.21 mmol) was added in one portion and left to react at 80 ^{0}C for 24 h. After cooling the reaction to room temperature, the solution was poured into distilled

water (3 x 100 mL). Sodium thiosulfate (3 x 120 mL) was added and the resulting yellow precipitate was collected by filtration under vacuum. The crude mixture was further purified by column chromatography (hexanes/ethyl acetate = 9:1) to obtain the pure product as a yellow solid (14.39 g, yield 65%). ^{1}H NMR (500 MHz, $CDCl_3$) δ 8.23 (s, 1H), 8.13 (s, 1H), 8.08 (d, *J* = 1.3 Hz, 1H), 7.79 - 7.78 (d, *J* = 8.7 Hz, 1H), 7.70 - 7.68 (dd, *J* = 8.7, 1.9 Hz, 1H), 3.96 -3.95 (d, *J* = 2.7 Hz, 6H). ^{13}C NMR (126 MHz, $CDCl_3$) δ 167.83, 167.73, 134.42, 132.06, 131.76, 130.68, 130.20, 130.13, 129.73, 128.97, 128.78, 122.99, 52.84, 52.80. HRMS Calcd for $C_{14}H_{11}BrO_4$ $[M+H]^+$: 322.9923. Found: 322.9913. Elem. Anal. calcd. for $C_{14}H_{11}BrO_4$: C, 52.04; H, 3.43. Found: C, 51.98; H, 3.35. m.p. 71 - 73 ℃.

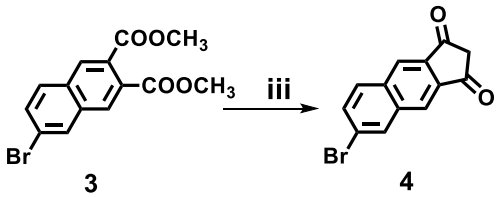

3 4

Synthesis of compound 4.

In a dry two-necked 10 mL flask, compound 3 (5.00 g, 15.47 mmol), NaH (0.63 g, 26.31 mmol), and 5 mL of dry ethyl acetate were mixed under N_2 atmosphere and heated to 80 ^{0}C for 5 h. After cooling the reaction to room temperature, the resulting light yellow precipitate was collected by filtration and washed with hexane (50 mL). The resulting solid was dissolved in hot water (100 mL) in about 3 h, next, the solution was acidified to a pH of 1-2 by slowly adding hydrochloric acid (2 M). The resulting precipitate was collected by filtration, washed with methanol, and dried in a vacuum oven to afford the pure target product as a light pink solid (1.92 g, yield 45%). ^{1}H NMR (500 MHz, $CDCl_3$) δ 8.49 (s, 1H), 8.41 (s, 1H), 8.29 (m, 1H), 8.80 - 7.98 (d, *J* = 8.9 Hz, 1H), 7.81 - 7.79 (dd, *J* = 8.8, 1.9 Hz, 1H), 3.38 (s, 2H). ^{13}C NMR (126 MHz, $CDCl_3$) δ 196.24, 196.15, 137.99, 137.43, 136.24, 133.72, 132.23, 131.52, 130.91, 123.42, 123.35, 122.17, 45.63. HRMS Calcd for $C_{13}H_7BrO_2$ $[M+H]^+$: 274.9690. Found: 274.9702. Elem. Anal. calcd. for $C_{13}H_7BrO_2$: C, 56.76; H, 2.56. Found: C, 56.60; H, 2.45. m.p. 174 - 176 ℃.

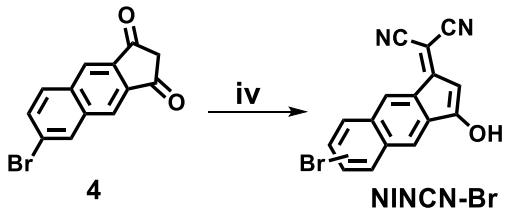

Synthesis of NINCN-Br.

In a dry two-necked 100 mL flask, compound 4 (1.02 g, 3.71 mmol), malononitrile (2.44 g, 37.10 mmol), and anhydrous sodium acetate (1.52 g, 18.54 mmol) were dissolved in dry ethanol (40 mL). The reaction mixture was stirred for 3 h at 50 ^{0}C before quenching it into ice water (100 mL). After acidification to a pH of 1-2 by the addition of hydrochloric acid (2 M), a precipitate formed, which was collected by filtration and washed with acetone. The crude solid was purified by column chromatography (hexanes/acetone = 1:3) to afford NINCN-Br as a dark red solid (0.84 g, yield 70%). ^{1}H NMR (500 MHz, THF-D8) δ 10.86 (s, 1H), 8.38 - 8.33 (d, 1H), 8.09 - 8.00 (m, 1H), 7.82 - 7.71 (m, 1H), 7.59 - 7.53 (m, 2H), 5.51 (s, 1H). ^{13}C NMR (126 MHz, THF-D8) δ 187.15, 186.93, 163.31, 163.00, 138.80, 138.76, 138.11, 136.24, 135.45, 135.26, 133.47, 132.64, 131.36, 130.95, 130.74, 130.26, 129.44, 120.21, 120.04, 119.85, 119.65, 119.30, 119.17, 119.04, 118.93, 117.14, 116.36, 106.01, 105.86. HRMS Calcd for $C_{16}H_7BrN_2O$ $[M-H]^-$: 320.9668. Found: 320.9669. Elem. Anal. calcd. for $C_{16}H_7BrN_2O$: C, 59.47; H, 2.18; N, 8.67. Found: C, 59.30; H, 2.09; N, 8.63. m.p. ＞ 370 ℃.

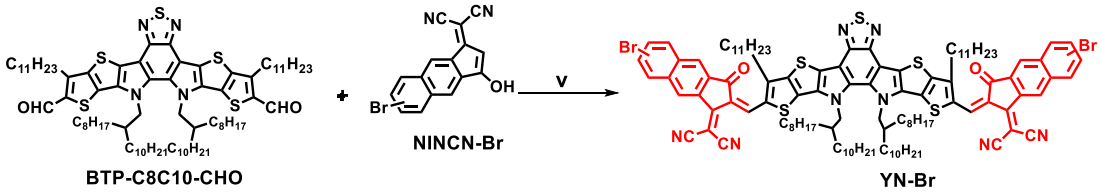

Synthesis of YN-Br.

BTP-C8C10-CHO (358.70 mg, 0.26 mmol), NIC-Br (445.91 mg, 1.31 mmol), chloroform (30 mL), pyridine (6 mL) and acetic acid (3 mL) were mixed into a two-necked 100 mL round-bottomed flask, and the system was deoxygenated by a N_2 flow for 10 min. The reaction mixture was stirred overnight at room temperature. After removing the solvent under vacuum, the resulting crude product was purified by column chromatography on silica gel using

chloroform as an eluent followed by recrystallization from chloroform/acetone to afford the pure YN-Br as a deep blue solid (415 mg, 80%). ^{1}H NMR (500 MHz, $CDCl_3$) δ 9.19 (d, *J* = 2.2 Hz, 1H), 9.15 (s, 1H), 9.10 (d, *J* = 2.2 Hz, 1H), 9.00 (s, 1H), 8.33 (s, 1H), 8.26 (d, *J* = 3.1 Hz, 1H), 8.19 (d, *J* = 2.1 Hz, 1H), 8.11 (s, 1H), 7.91 - 7.88 (m, 2H), 7.78 -7.71 (m, 2H), 4.84 (d, *J* = 6.3 Hz, 4H), 3.21-3.11 (m, 4H), 2.20-2.17 (m, 2H), 1.92 - 1.78 (m, 4H), 1.66 - 0.92 (m, 96H), 0.88 - 0.75 (m, 18H). ^{13}C NMR (126 MHz, $CDCl_3$) δ 187.85, 187.81, 160.24, 160.12, 153.90, 153.81, 147.53, 145.39, 137.88, 137.01, 136.40, 136.17, 135.83, 135.60, 135.48, 135.20, 134.55, 134.23, 134.15, 134.11, 133.93, 133.60, 133.33, 133.04, 132.86, 132.44, 132.01, 131.85, 131.28, 131.06, 131.02, 126.49, 125.35, 124.48, 124.09, 123.96, 122.93, 122.37, 115.82, 115.77, 115.57, 115.50, 113.71, 67.29, 66.94, 55.85, 39.23, 31.95, 31.94, 31.90, 31.25, 31.22, 30.67, 29.90, 29.88, 29.79, 29.73, 29.70, 29.65, 29.57, 29.53, 29.49, 29.45, 29.44, 29.40, 29.37, 29.30, 29.28, 25.73, 22.70, 22.67, 22.65, 14.13, 14.12. HRMS Calcd for $C_{114}H_{140}Br_2N_8O_2S_5$ $[M+H]^+$: 1971.8141. Found: 1971.8142. Elem. Anal. calcd. for $C_{114}H_{140}Br_2N_8O_2S_5$: C, 69.35; H, 7.15; N, 5.68. Found: C, 69.23; H, 7.13; N, 5.63. m.p. 268 - 270 °C.

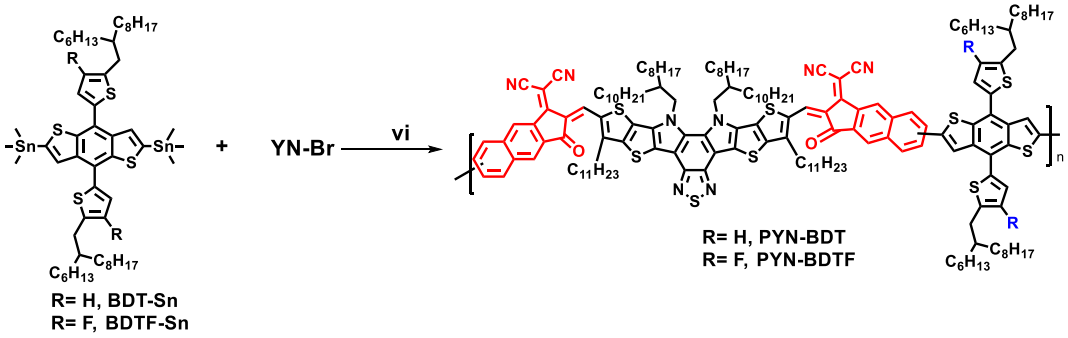

Synthesis of PYN-BDT.

In a dry two-necked 10 mL flask, YN-Br (123.77 mg, 0.06 mmol), the BDT-Sn (70.77 mg, 0.06 mmol) and $Pd(PPh_3)_4$ (5.00 mg, 0.004 mmol) were dissolved in dried toluene (5 mL) under N_2. The mixture was bubbled with N_2 for 10 min and then slowly heated to 110 °C for 3 h. After cooling to room temperature, the solution was slowly added to methanol and the resulting precipitates were collected by filtration and washed in a Soxhlet extractor with methanol, hexane, acetone, dichloromethane, and chloroform. The chloroform fraction was precipitated

with methanol, dried under vacuum at 50 °C overnight to obtain the polymer acceptor PYN-BDT (110.00 mg, 67 %). ^{1}H NMR (600 MHz, $C_2D_2Cl_4$) δ 9.40 - 9.15 (m, 4H), 8.52 - 7.32 (m, 14H), 7.16 - 6.92 (m, 2H), 4.89 (s, 5H), 3.49 - 2.80 (m, 9H), 2.22 - 1.87 (m, 8H), 1.74 - 0.33 (m, 170H). Elem. Anal. calcd. for $[C_{164}H_{214}N_8O_2S_9]_n$: C, 75.24; H, 8.24; N, 4.28. Found: C, 75.10; H, 8.08; N, 4.10.

Synthesis of PYN-BDTF.

The synthesis of PYN-BDTF was similar to the PYN-BDT polymer with a yield of 70%. ^{1}H NMR (600 MHz, $C_2D_2Cl_4$) δ 9.46 - 9.08 (m, 4H), 8.56 - 7.65 (m, 11H), 7.35 (d, J = 46.9 Hz, 2H), 4.89 (s, 4H), 3.35 (s, 4H), 2.96 (d, J = 34.0 Hz, 4H), 2.22 (s, 2H), 2.13 - 1.78 (m, 6H), 1.76 - 0.38 (m, 173H). Elem. Anal. calcd. for $[C_{164}H_{212}F_2N_8O_2S_9]_n$: C, 74.22; H, 8.05; N, 4.22. Found: C, 73.89; H, 8.22; N, 4.03.

3. Polymer Characterization

UV-vis spectra were recorded on a Varian Cary 100 and a Perkin Elmer LAMBDA 1050 UV-vis spectrophotometer. The PL spectra were measured on a Horiba Nanolog spectrofluorimeter(FL3-2iHR/iHR) instrument. The PL quenching efficiencies stated in Figure 4d were estimated by the ratio of the emission intensities of the pristine and blend films. One should note that, though the excitation intensities remained constant, the emission intensities might still be influenced by the difference of the thickness, the excitation angle and the inhomogeneity of the films. The solutions were prepared with a concentration of 0.01 mg/mL in chloroform and measured at ambient temperature. Thin films were cast from chloroform (7.0 mg/mL, 3000 rpm) onto glass slides.

Cyclic voltammograms (CV) were acquired using a CHI760E voltammetric analyzer and measured with a three-electrode system using a disk Pt working electrode, an Ag/AgCl reference electrode, and a platinum wire counter electrode in acetonitrile solution of tetrabutylammonium hexafluorophosphate (n-Bu_4NPF_6), and ferrocene/ferrocenium (Fc/Fc^+) was used as an internal reference. Thermogravimetric Analysis (TGA) measurements were carried out on Mettler Toledo TGA/DSC 3+ instrument, the scanning rate is 10 ^{0}C/min from

50 to 600 ^{0}C, and Differential Scanning Calorimetry (DSC) measurements were performed on an indium-calibrated Mettler-Toledo DSC822e equipped with a TSO801RO autosampler. The samples were placed in lidded 40 μL Al pans and thermally cycled twice under nitrogen with a heating/cooling rate of 10 °C/min. The reported data correspond to the first cooling cycle and second warming cycle.

The EQE measurements to correct the photocurrent were recorded on an Oriel model QE-PV-SI instrument in the air at ambient temperature. For all the device characterization, no preconditioning was applied.

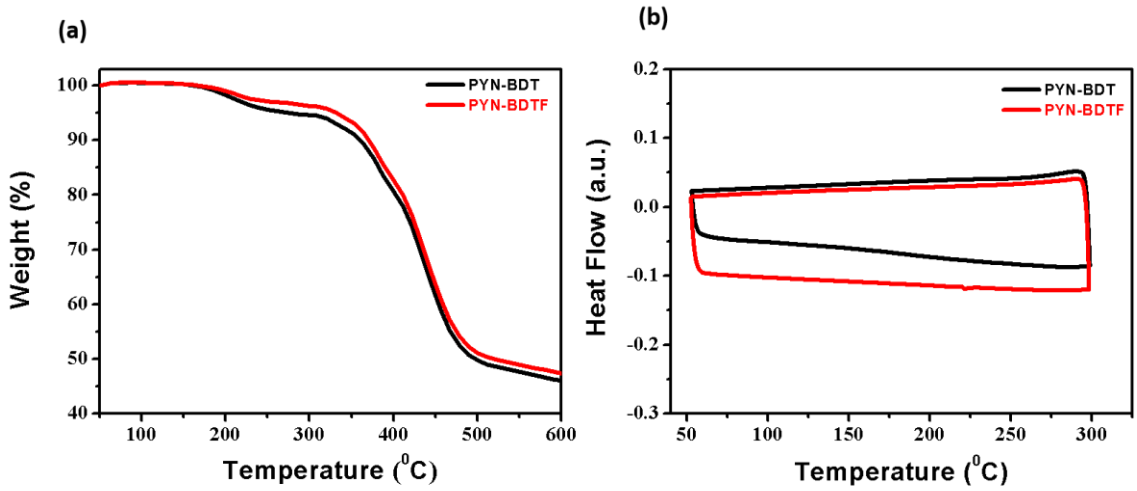

Figure S1. (a) TGA and (b) DSC plots of PYN-BDT and PYN-BDTF.

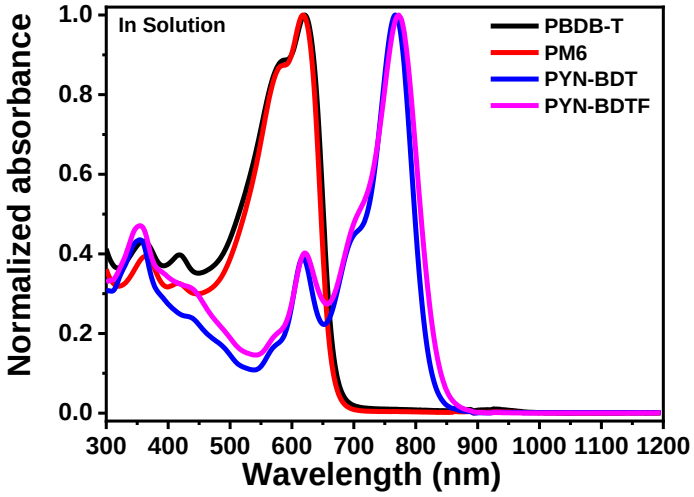

Figure S2. UV-Vis optical absorption spectra of PBDB-T, PM6, PYN-BDT and PYN-BDTF in

solution.

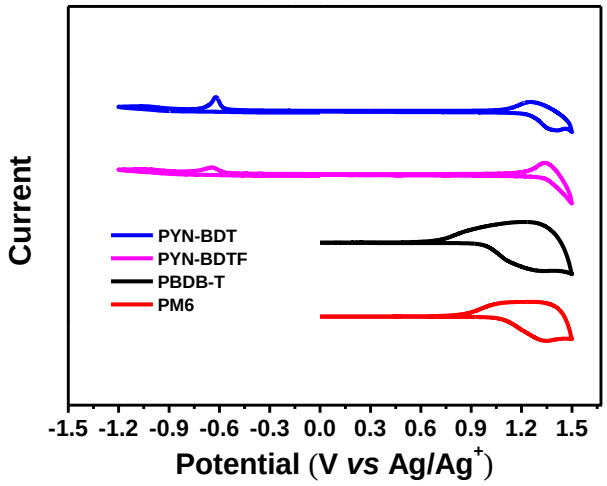

Figure S3. Cyclic voltammetry scans of PBDB-T, PM6, PYN-BDT, and PYN-BDTF films.

4. Morphology and Microstructure Analysis

Grazing-incidence wide-angle x-ray scattering (GIWAXS) measurements were performed at beamLine 8ID-E at the Advanced Photon Source at Argonne National Laboratory. The samples were irradiated at incidence angles from 0.130° to 0.140° in vacuum at 10.915 keV for two summed exposures of 2.5 s each. Signals were collected with a Pilatus 1M detector located at a distance of 228.16 mm from the samples. Blend films for GIWAXS were prepared according to the procedure for photovoltaic devices. For neat films, 14 mg mL^{-1} solutions of corresponding polymers in chloroform were used to cast on Si (20 mm x 20 mm).

Atomic force microscopy (AFM) was measured on a Dimension Icon scanning probe microscope (Bruker Dimension FastScan AFM) in standard tapping mode. The blend thin films were prepared in the same way as the photovoltaic devices and spun cast on Si substrates. The neat films were spun cast on Si substrates in chloroform 14 mg/mL solutions.

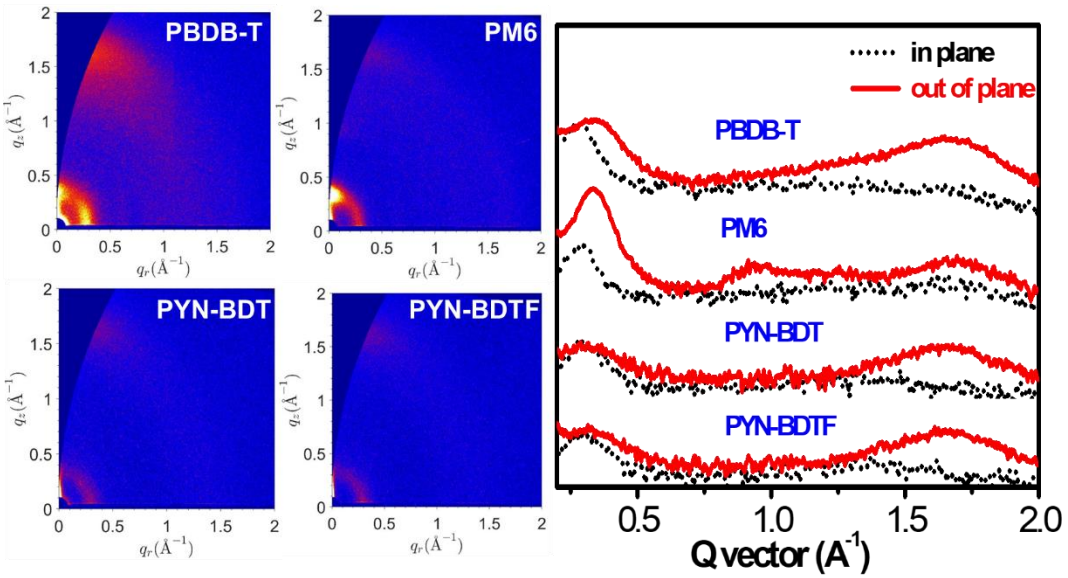

Figure S4. 2D GIWAXS patterns of PBDB-T, PM6, PYN-BDT and PYN-BDTF neat films.

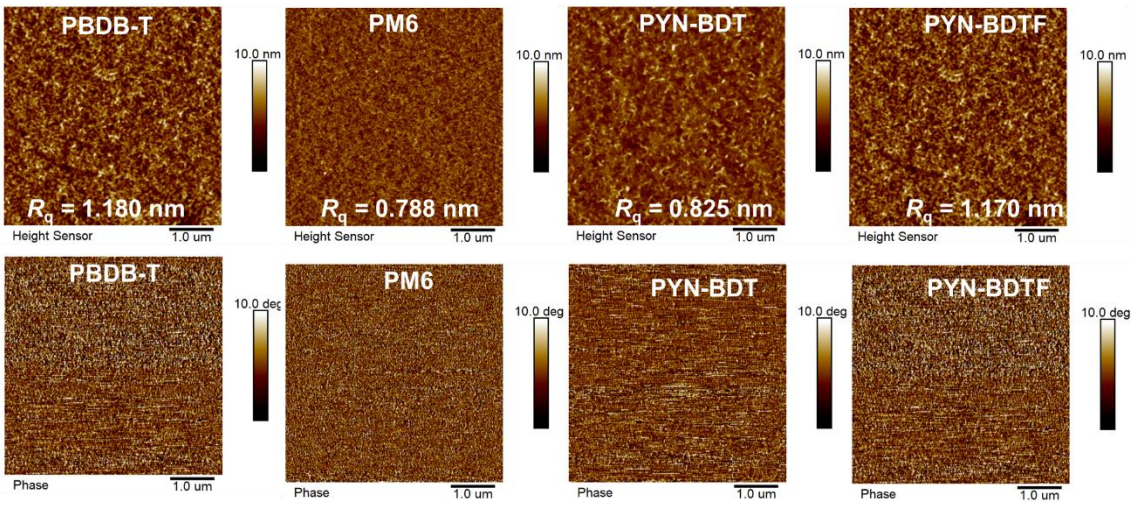

Figure S5. AFM height (top) and phase (bottom) images of PBDB-T, PM6, PYN-BDT, and PYN-BDTF neat films.

Table S1. Summary of reflection position, d-spacing, and correlation length (CL) of the indicated films from GIWAXS measurements.

Sample	(100)			(010)		
	Position ($Å^{-1}$)	d-spacing (Å)	CL (Å)	Position ($Å^{-1}$)	d-spacing (Å)	CL (Å)
PBDB-T	0.29	21.7	56.1	1.72	3.65	28.1

PM6	0.29	21.7	51.1	1.71	3.67	17.1
PYN-BDT	0.30	20.9	43.2	1.70	3.69	22.5
PYN-BDTF	0.30	20.9	46.8	1.69	3.71	24.4
PBDB-T:PYN-BDT	0.30	20.9	70.3	1.72	3.65	22.5
PBDB-T:PYN-BDTF	0.30	20.9	62.4	1.70	3.67	25.5
PM6:PYN-BDT	0.30	20.9	66.1	1.70	3.67	19.6
PM6:PYN-BDTF	0.30	20.9	73.9	1.70	3.67	21.6

5. Solar Cell Device Fabrication and Characterization

Solar cells were fabricated in a conventional device configuration of ITO/PEDOT:PSS/active layers/PNDIT-F3N/Ag. The ITO substrates were scrubbed with detergent and then sonicated with deionized water, acetone, and isopropanol, then subsequently dried overnight in an oven. The glass substrates were treated with UV-ozone for 30 min before use. PEDOT:PSS (Heraeus Clevios P VP AI 4083) was spin-cast onto the ITO substrates at 4000 rpm for 30 s, and then dried at 150 °C for 15 min in air. The donor : acceptor blends (1:1 weight ratio) were dissolved in chloroform (total concentration = 11.5 mg/mL for blend), in which 1-chloronaphthalene (CN) was also added in 3 vol% as an additive, and stirred overnight in a nitrogen-filled glove box. The solution was then spin-cast at 2300 rpm for 30 s onto PEDOT:PSS film, after being kept on a 65 °C hotplate for 30 min. Then, the active layers were placed in a vacuum chamber to remove extra CN in the films before they went through a 100 °C temperature annealing for 5 min. A thin PNDIT-F3N layer was coated on the active layer, followed by the deposition of Ag (evaporated under 5×10^{-4} Pa through a shadow mask). The optimal active layer thickness measured by a Bruker Dektak XT stylus profilometer was about 110 nm. The current density-voltage (*J-V*) curves of all encapsulated devices were measured using a Keithley 2400 Source Meter in the air under AM 1.5G (100 mW cm^{-2}) using a Newport solar simulator. The light intensity was calibrated using a standard Si diode (with KG5 filter, purchased from PV Measurements to bring spectral mismatch to unity). An optical microscope (Olympus BX51)

was used to define the device area (5.9 mm^2). EQEs were measured using an Enlitech QE-S EQE system equipped with a standard Si diode. Monochromatic light was generated from a Newport 300W lamp source.

Devices with an inverted device architecture of ITO /ZnO (~25 nm) /Active layer(90 -100 nm) /MoO_3 (10 nm)/Ag (100 nm) were also fabricated. Pre-patterned ITO-coated glass wafers (Thin Film Devices, Inc.) with a sheet resistance of ≈ 20 Ω/sq were used as substrates. The ZnO precursor solution is prepared by dissolving 220 mg of zinc acetate dehydrate (Sigma Aldrich) and 62 mg of 2-ethanolamine (Sigma Aldrich) in 2 mL 2-methoxyethanol (Sigma Aldrich), then stir overnight. The ZnO precursor is spin-coated on precleaned ITO glass at 7000 rpm after filtering through a 0.45 μm PVDF filter and 20 min at 170°C in air. Then the device is transferred into an argon glove box. After that, active layer solutions (11.5 mg/mL in total) were then spin-coated onto the ZnO layer (Argon filled glovebox) while spinning 3000 RPM depending on viscosity to achieve appropriate thicknesses of 90~100 nm. All the substrates were loaded into a metal-evaporation chamber and with a mask of dimensions of mm^2. Then these substrates were vapor-deposited with a molybdenum oxide interlayer (10 nm) and silver (100 nm) electrode at high vacuum (~6 x 10^{-6} Torr). All the devices were measured under simulated AM1.5G irradiation (100 mW cm^{-2}) illumination with a standard ABET Sun 2000 Solar Simulator in the air. A standard silicon solar cell was used to calibrate the light intensity. The voltage was scanned from 1.20 V to -0.20 V. The external quantum efficiency (EQE) is measured by the Newport QE-PV-SI setup in the air. A calibrated silicon solar cell was used as a reference.

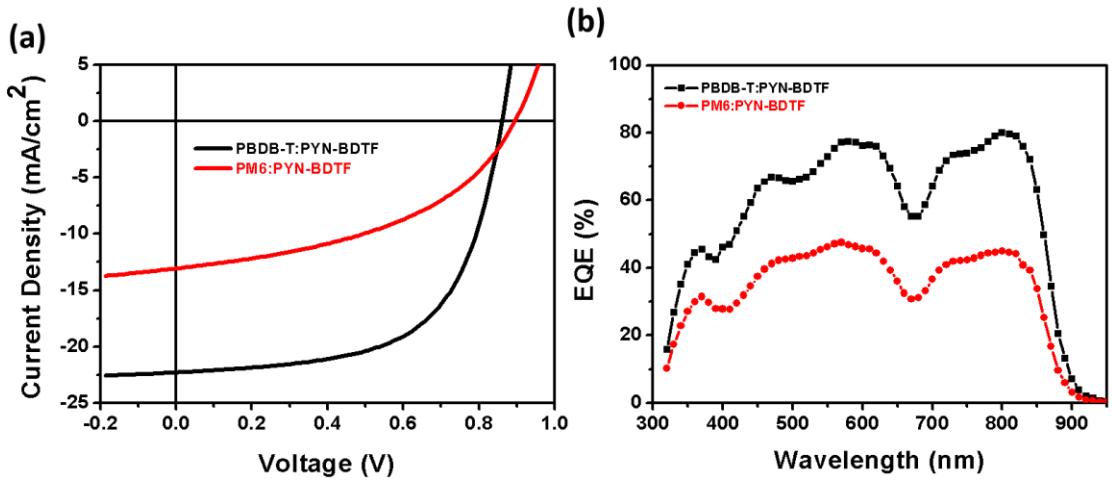

Figure S6. *J-V* characteristics of APSCs based on PBDB-T:PYN-BDTF and PM6:PYN-BDTF blend films using inverted devices. (B) EQE curves of corresponding APSCs.

6. Charge Transport Measurements

The hole and electron mobilities were measured by the space charge limited current (SCLC) technique using the following diode architectures: 1. Hole-only devices: Glass/ITO/PEDOT: PSS (30 nm)/active layer (90 - 100 nm)/MoO_3 (10 nm) /Ag (100 nm). 2. Electron-only devices: Glass/ITO/ZnO(~ 25 nm)/active layer (90 - 100 nm)/PNDIT-F3N (5 nm)/Ag (100 nm). The blend was deposited as described according to the procedure for photovoltaic devices. The SCLC mobilities were calculated by the Mott-Gurney equation:

$$J = \frac{9}{8}\varepsilon_0\varepsilon_r\mu\frac{V^2}{d^3}$$

where J is the current density, ε_r is the dielectric constant of the active layer, ε_0 is the vacuum permittivity, μ is the mobility of hole or electron and d is the thickness of the active layer, V is the internal voltage in the device, and $V = V_{appl} - V_{bi}$, where V_{appl} is the voltage applied to the device, and V_{bi} is the built-in voltage resulting from the relative work function difference between the two electrodes. J_{ph} is related to the current density under the illumination of 100 mW cm $^{-2}$ (J_L) and in the dark (J_D) which is defined as $J_{ph} = J_L - J_D$. V_{eff} is determined from the voltage at when $J_{ph} = 0$ (V_0) and the applied voltage (V_a) and is defined as $V_{eff} = V_0 - V_a$.

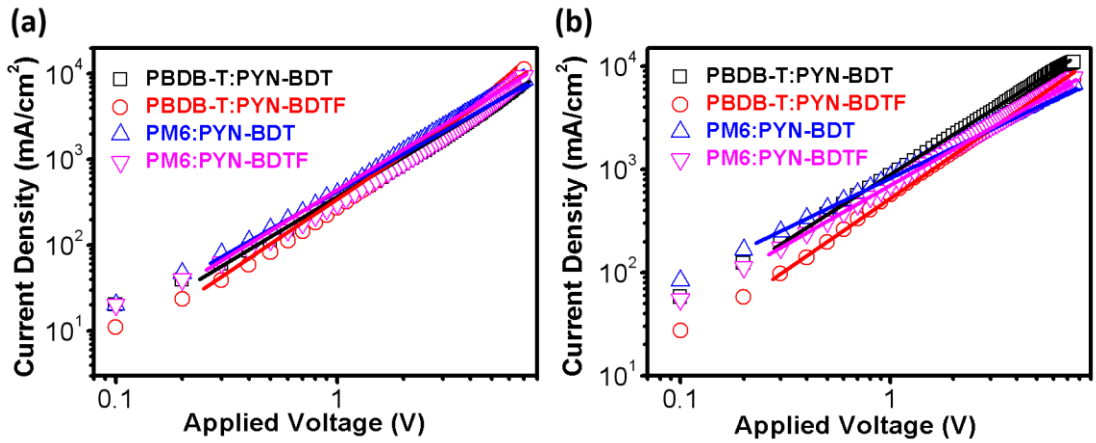

Figure S7. Current-voltage plots of (a) hole-only and (b) electron-only devices.

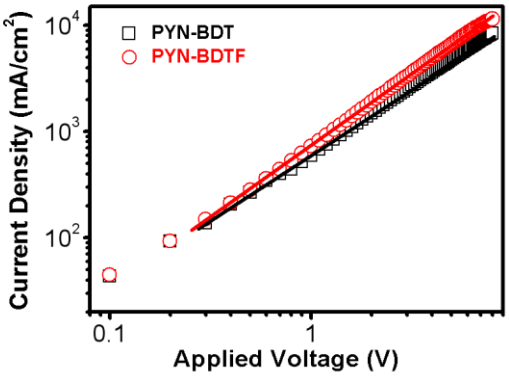

Figure S8. Current-voltage plots of PYN-BDT and PYN-BDTF, electron-only.

Table S2. Charge transport parameters of the indicated neat and blend films.

Sample	Hole mobility (10^{-4} cm^2 V^{-1} s^{-1})	Electron mobility (10^{-4} cm^2 V^{-1} s^{-1})
PBDB-T:PYN-BDT	8.84	4.65
PBDB-T:PYN-BDTF	9.39	5.52
PM6:PYN-BDT	8.33	3.33
PM6:PYN-BDTF	8.52	4.05
PYN-BDT	-	6.94

Table S3. Key photovoltaic parameters calculated from the J_{ph} - V_{eff} curves of the indicated four devices.

Samples	J_{sat} (mA/cm^2)	J_{ph}^b (mA/cm^2)	J_{ph}^c (mA/cm^2)	J_{ph}^b/J_{sat} (%)	J_{ph}^c/J_{sat} (%)
PBDB-T:PYN-BDT	23.965	21.326	17.515	89.0	73.1
PBDB-T:PYN-BDTF	24.486	22.282	19.287	90.9	78.7
PM6:PYN-BDT	17.110	14.356	9.649	83.9	56.4
PM6:PYN-BDTF	19.301	16.596	12.316	86.0	63.8

[b] Measured at under short-circuit conditions; [c] Measured at the maximal power output conditions.

7. Integrated Photocurrent Device Analysis

PBDB-T:PYN-BDTF and PM6:PYN-BDTF inverted solar cells were measured in ambient conditions using variable illumination intensities via an optical density filter wheel, as described earlier.[2] Photocurrent ($J_{pc} = J - J_{dark}$) characteristics in Figure S9 were obtained by measuring current-voltage (J-V) characteristics using a Keithley 2400 source-measurement unit. Carrier mobility in Figure S10 is effective average mobility ($\mu_{eff} = (\mu_e + \mu_h)/2$) at maximum power point and thus does not need to match the mobility values from SCLC measurements. Bias and intensity-dependent impedance measurements were carried out by a Solartron 1260 impedance analyzer using an AC amplitude of 100 mV while varying the frequency in the range of 100 Hz to 5 MHz. The impedance analyzer was controlled by a ZPlot/ZView software from Scribner Associates, Inc. All hardware components, LabView programs, and ZPlot programs were controlled by a homemade Autoit script (https://www.autoitscript.com/site/) for full automation of IPDA measurements. The data analyses were conducted in IGOR software, Flexible Electronics Data Management System (FlexEDMS) that is publicly available at https://github.com/MikeHeiber/FlexEDMS

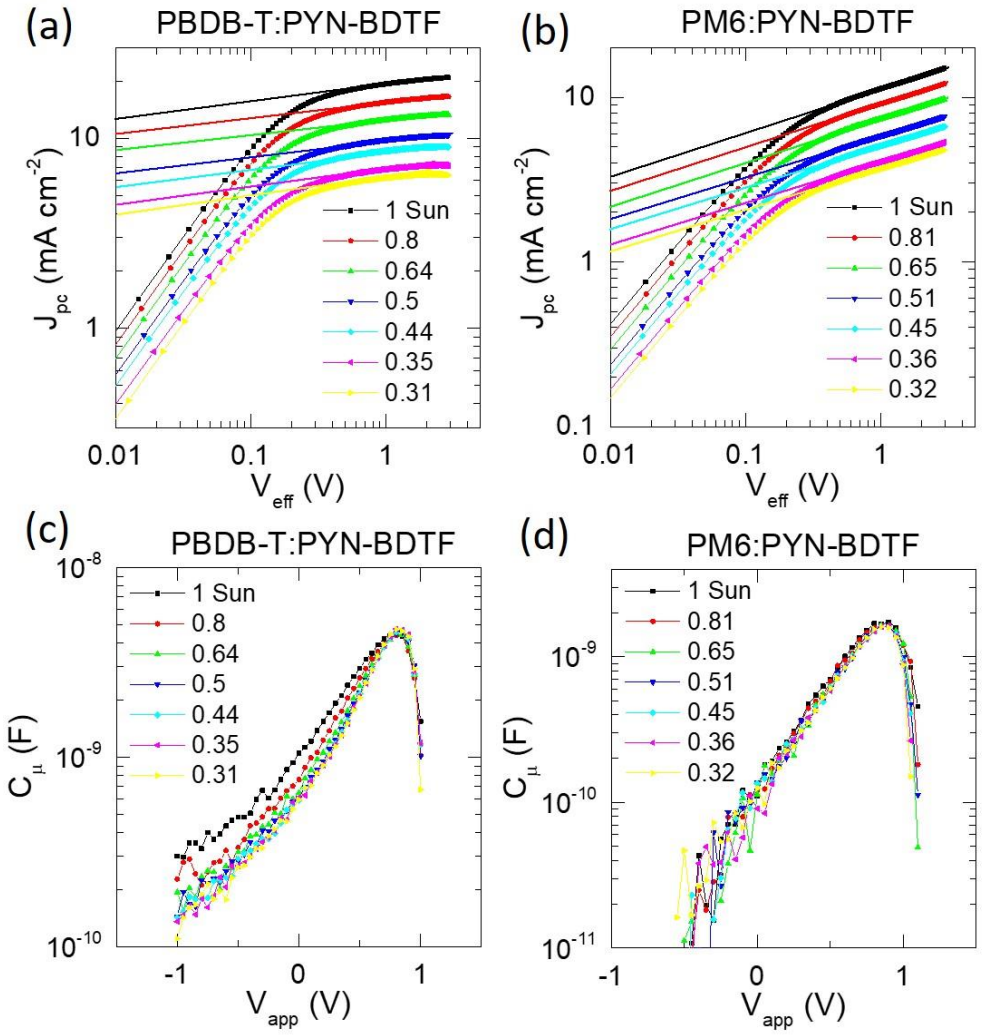

Figure S9. (a) Photocurrent density (J_{pc}) versus effective voltage (V_{eff}) for an inverted PBDB-T:PYN-BDTF cell under varying illumination intensity. (b) J_{pc} versus V_{eff} for an inverted PM6:PYN-BDTF cell under varying illumination intensity. (c), (d) C_{μ} versus V_{app} for the same PBDB-T:PYN-BDTF and PM6:PYN-BDTF cells. The data for (a) – (d) was used for IPDA analysis to extract device parameters shown in Figure 5 of main text and Figure S10.

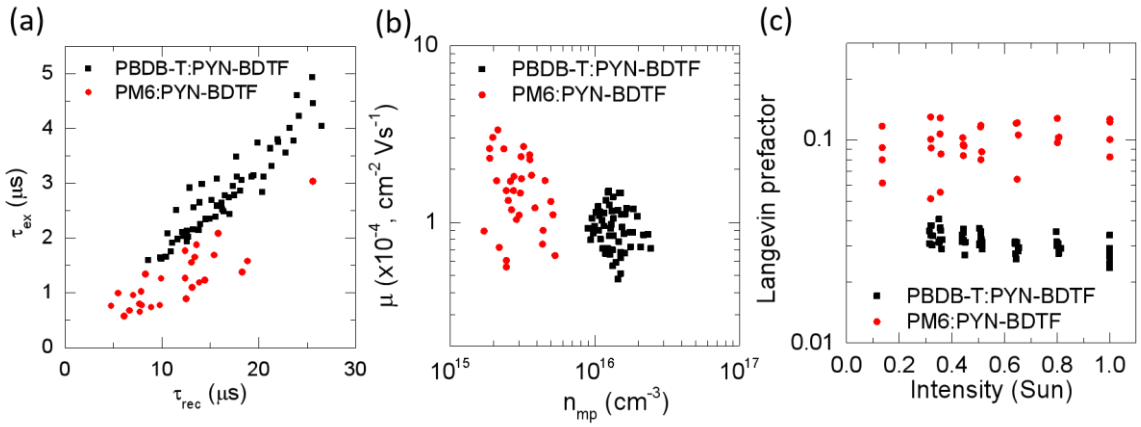

Figure S10. (a) Extraction time (τ_{ex}) and recombination lifetime (τ_{rec}) of the same cells. (b) Carrier mobility (μ) versus carrier density at maximum power point (n_{mp}) for PBDB-T:PYN-BDTF and PM6:PYN-BDTF cell. (c) Langevin prefactor versus illumination intensity for the same cells.

8. ^{1}H NMR and ^{13}C NMR Spectra

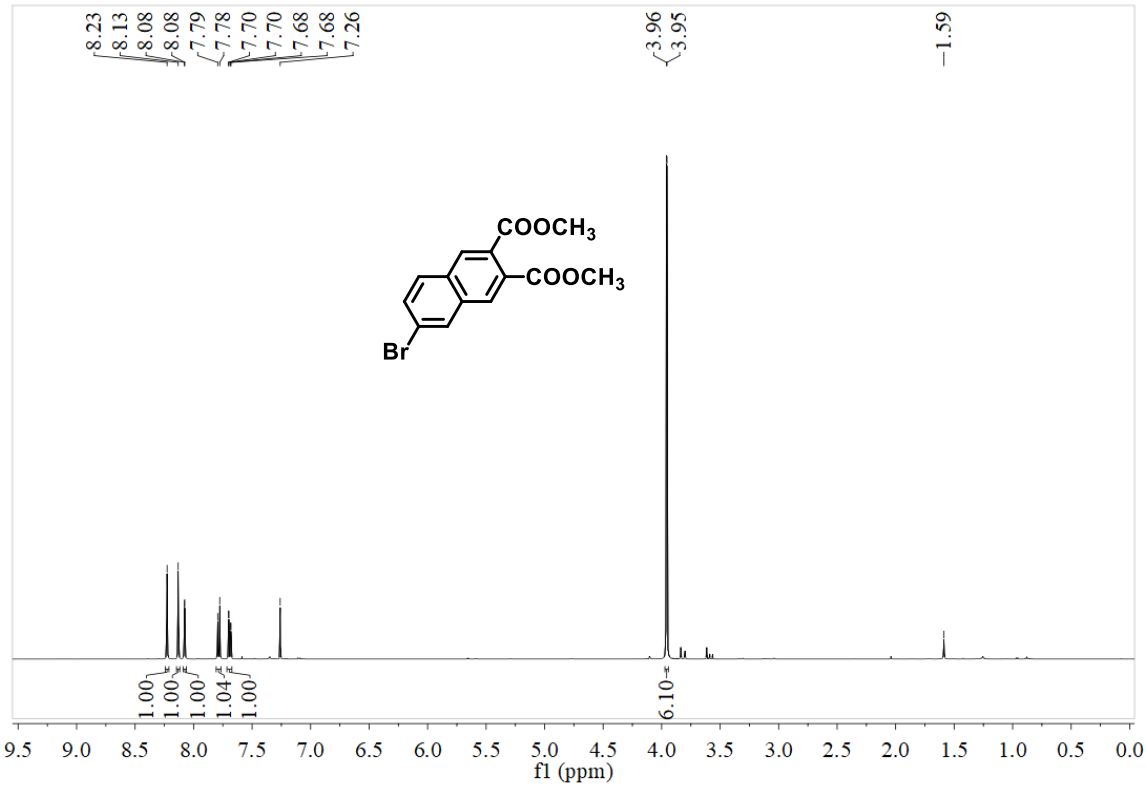

Figure S11. ^{1}H NMR of compound 3 in $CDCl_3$.

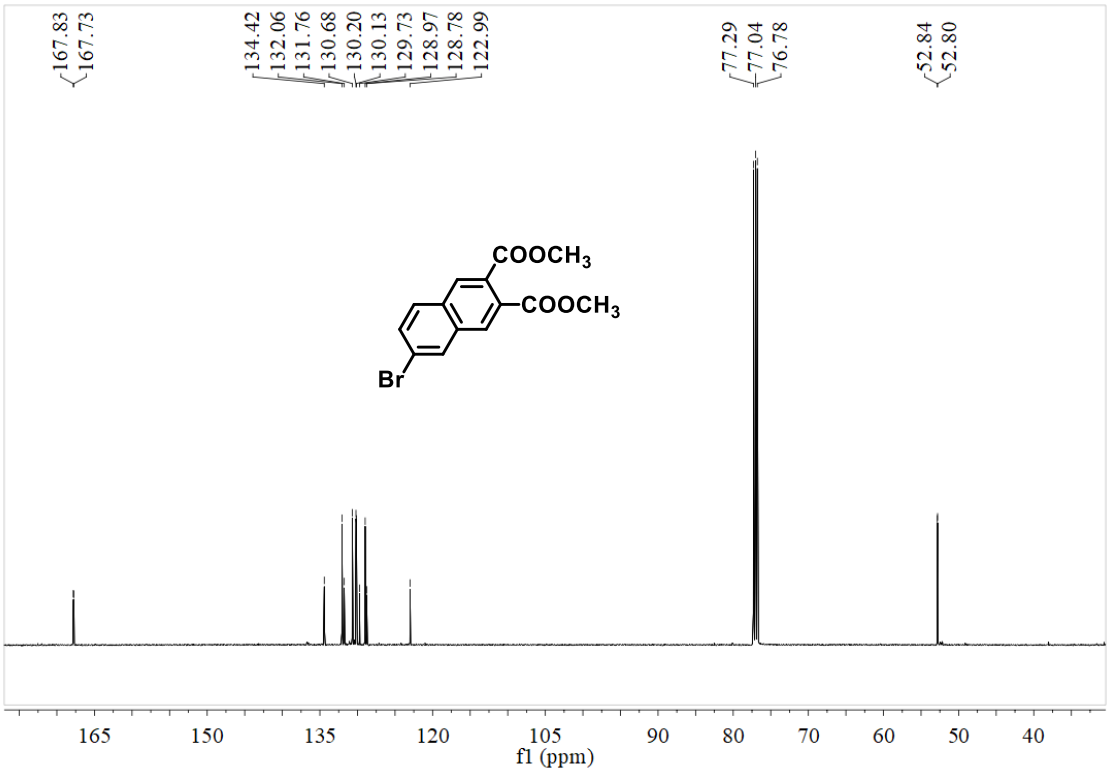

Figure S12. ^{13}C NMR of compound 3 in $CDCl_3$.

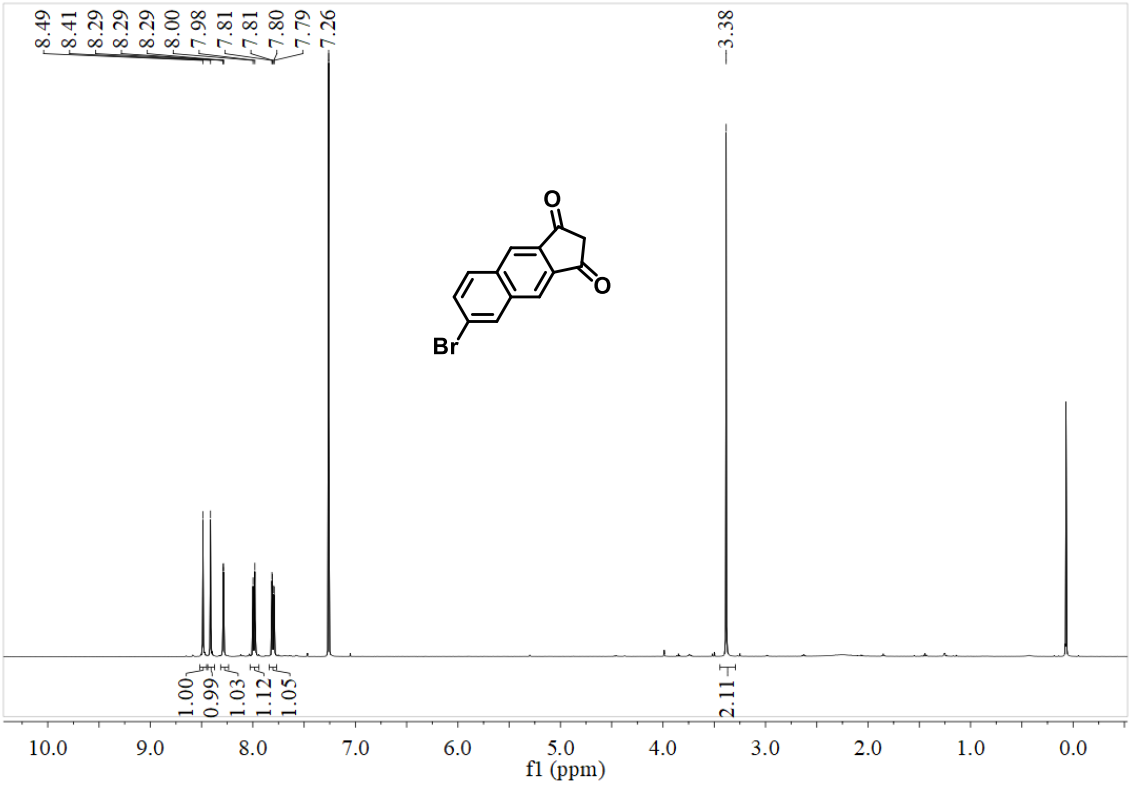

Figure S13. ^{1}H NMR of compound 4 in $CDCl_3$.

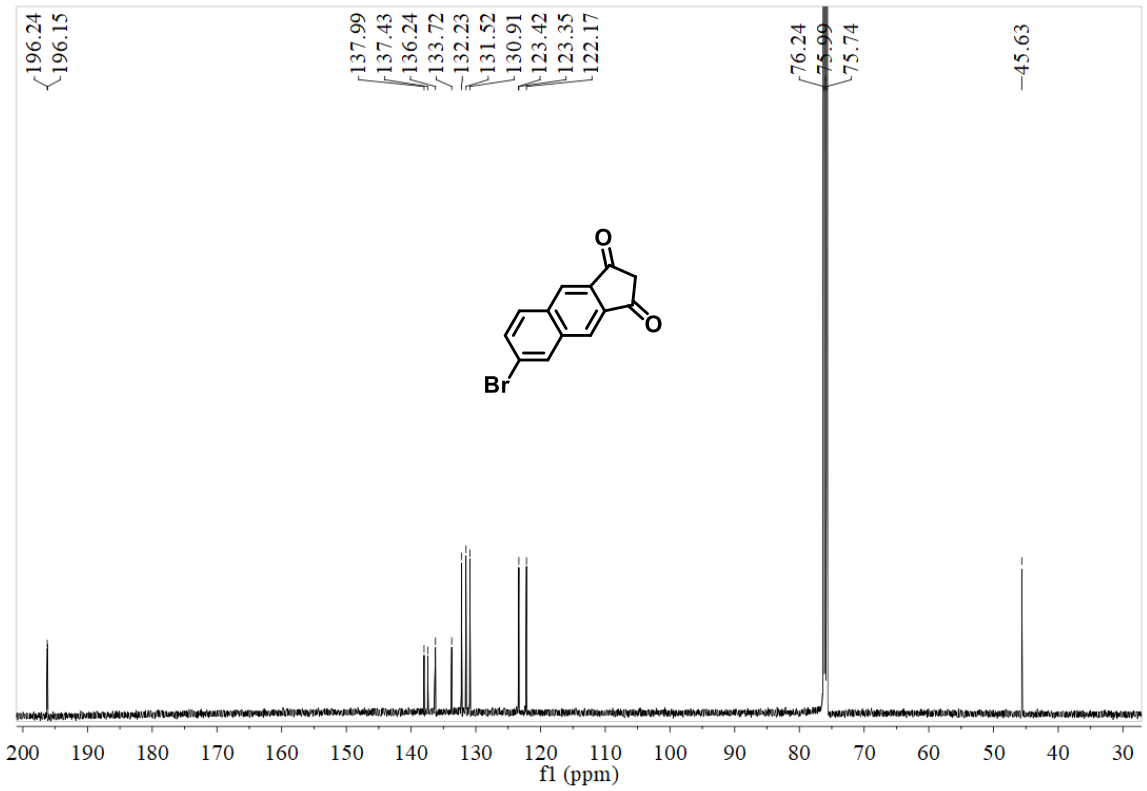

Figure S14. ^{13}C NMR of compound 4 in $CDCl_3$.

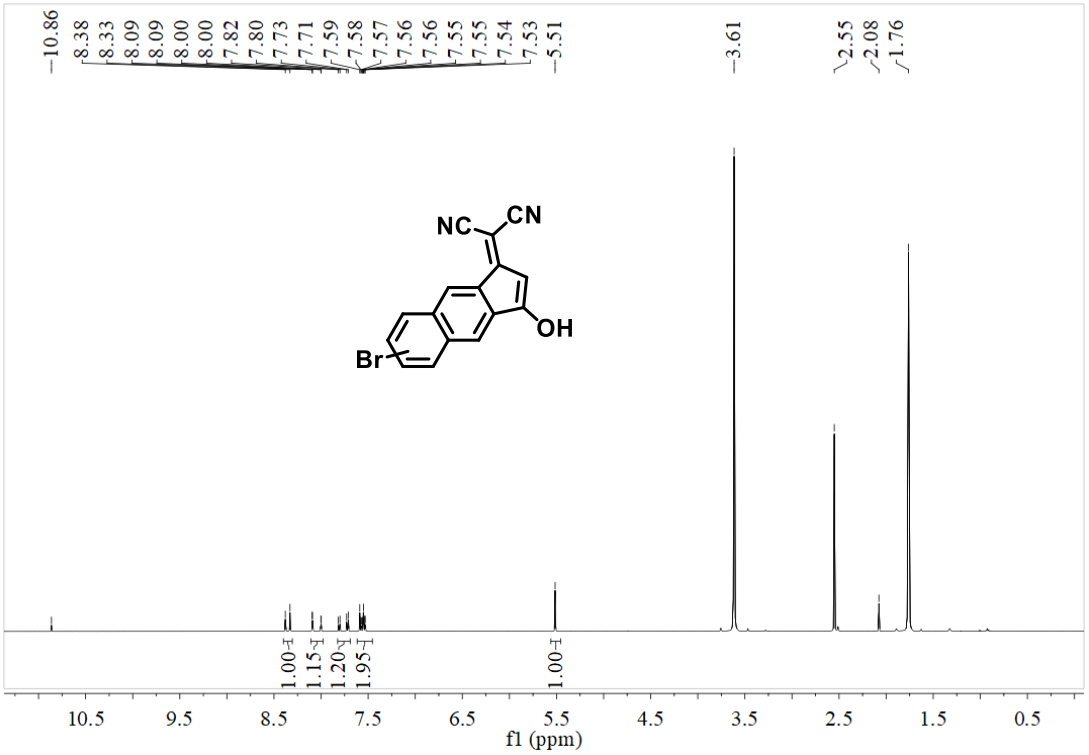

Figure S15. ^{1}H NMR of compound 5 in THF-D8.

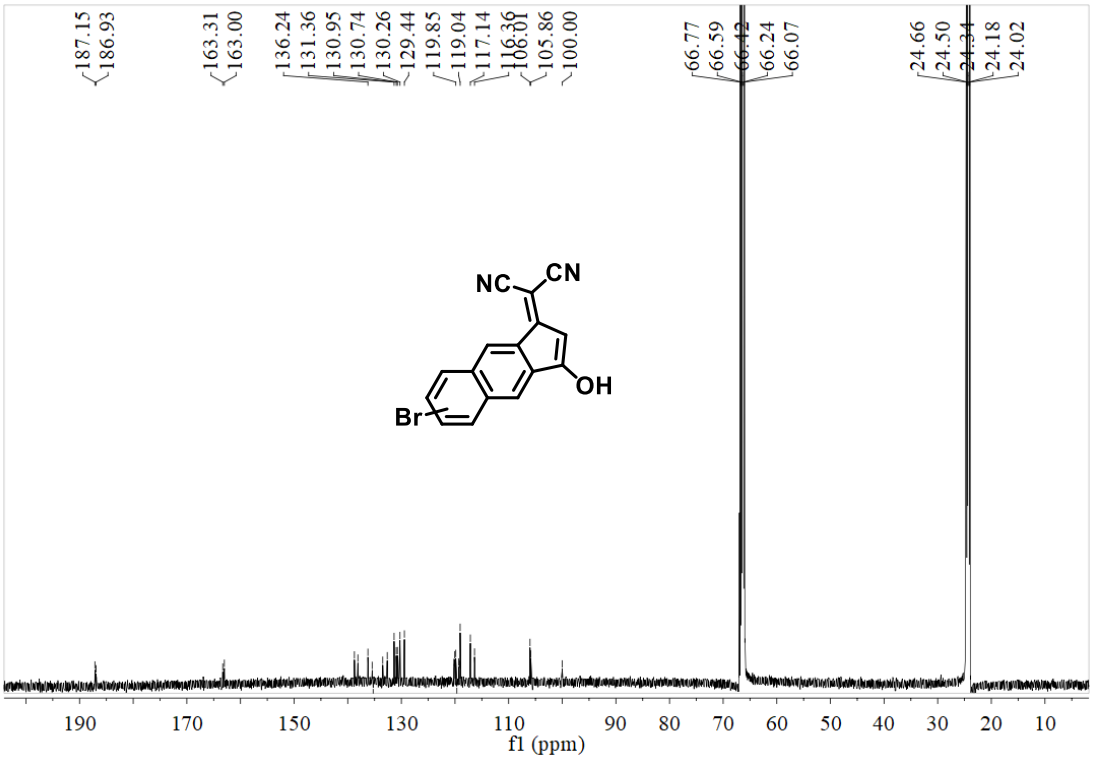

Figure S16. ^{13}C NMR of compound 5 in THF-D8.

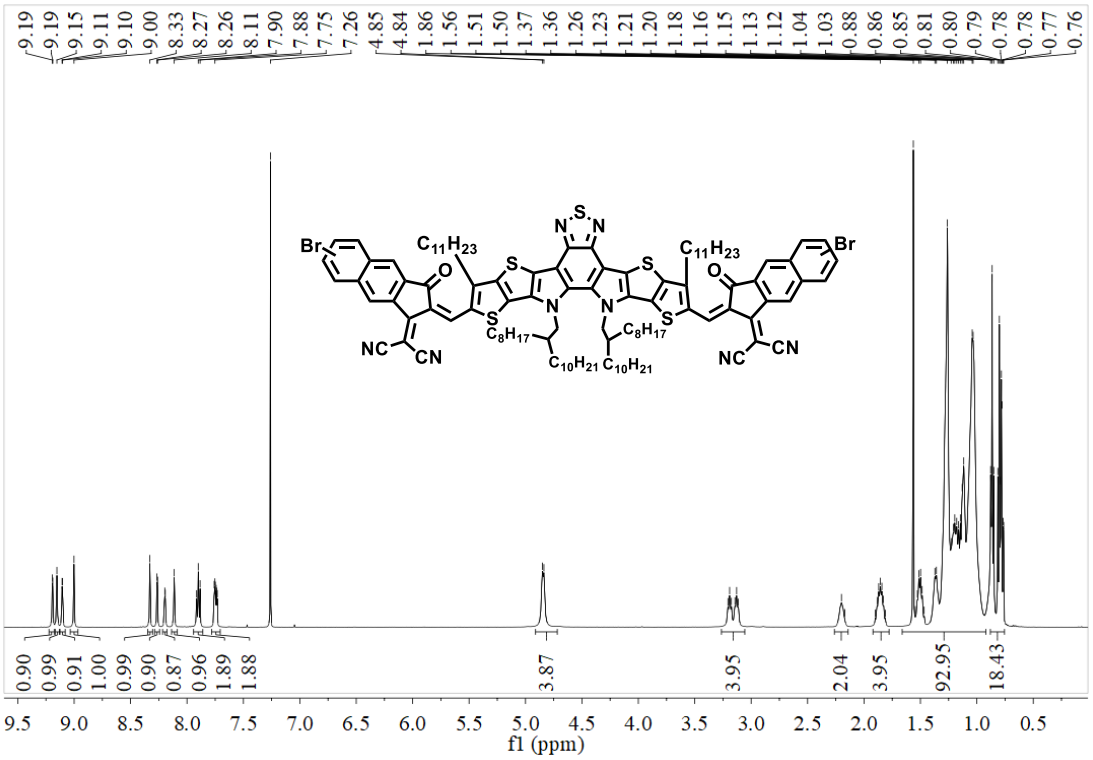

Figure S17. ^{1}H NMR of YN-Br in $CDCl_3$.

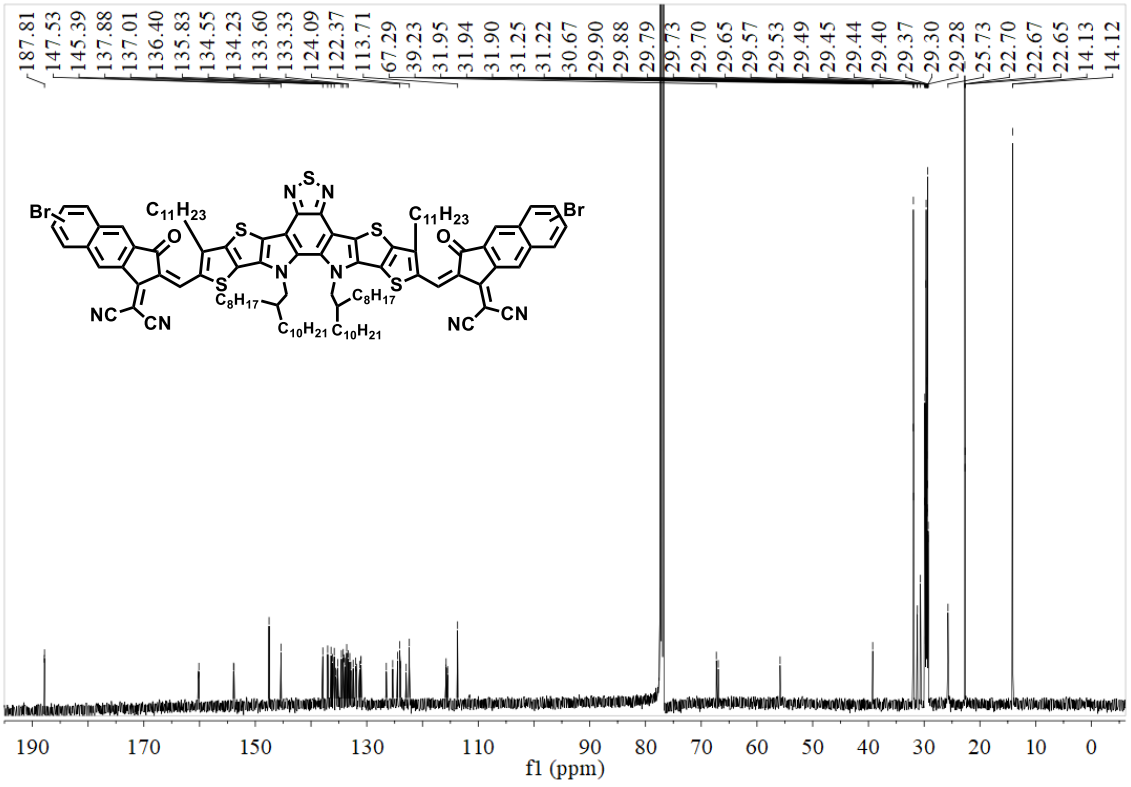

Figure S18. ^{13}C NMR of YN-Br in $CDCl_3$.

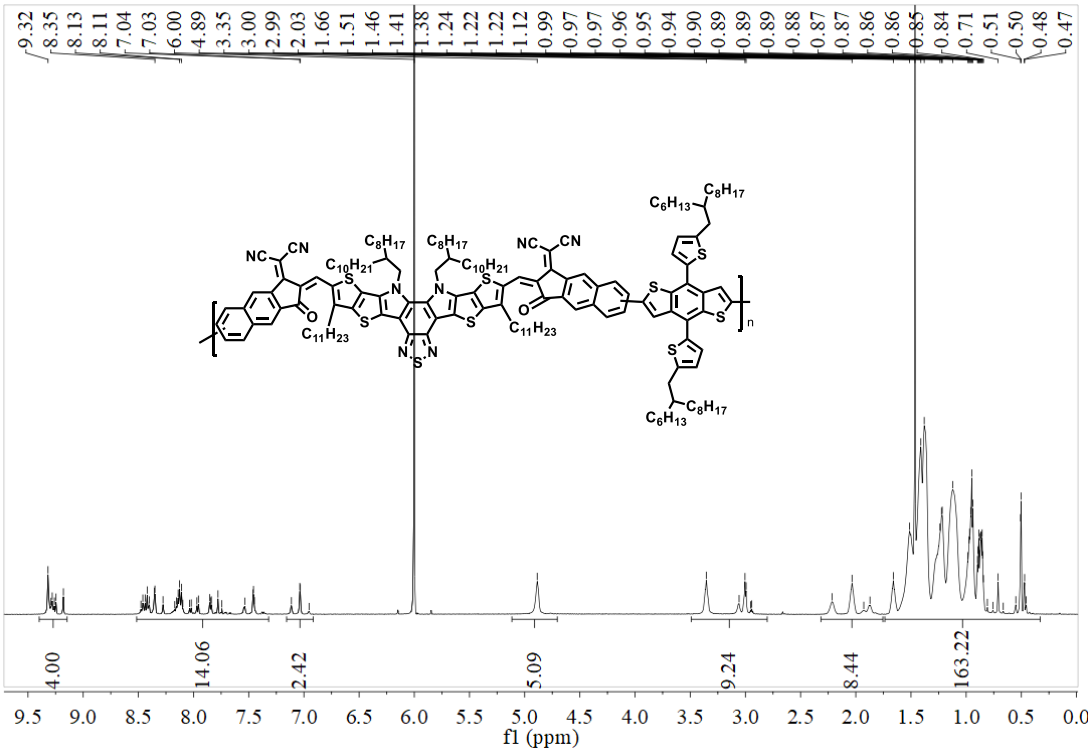

Figure S19. ^{1}H NMR of PYN-BDT in $C_2D_2Cl_4$.

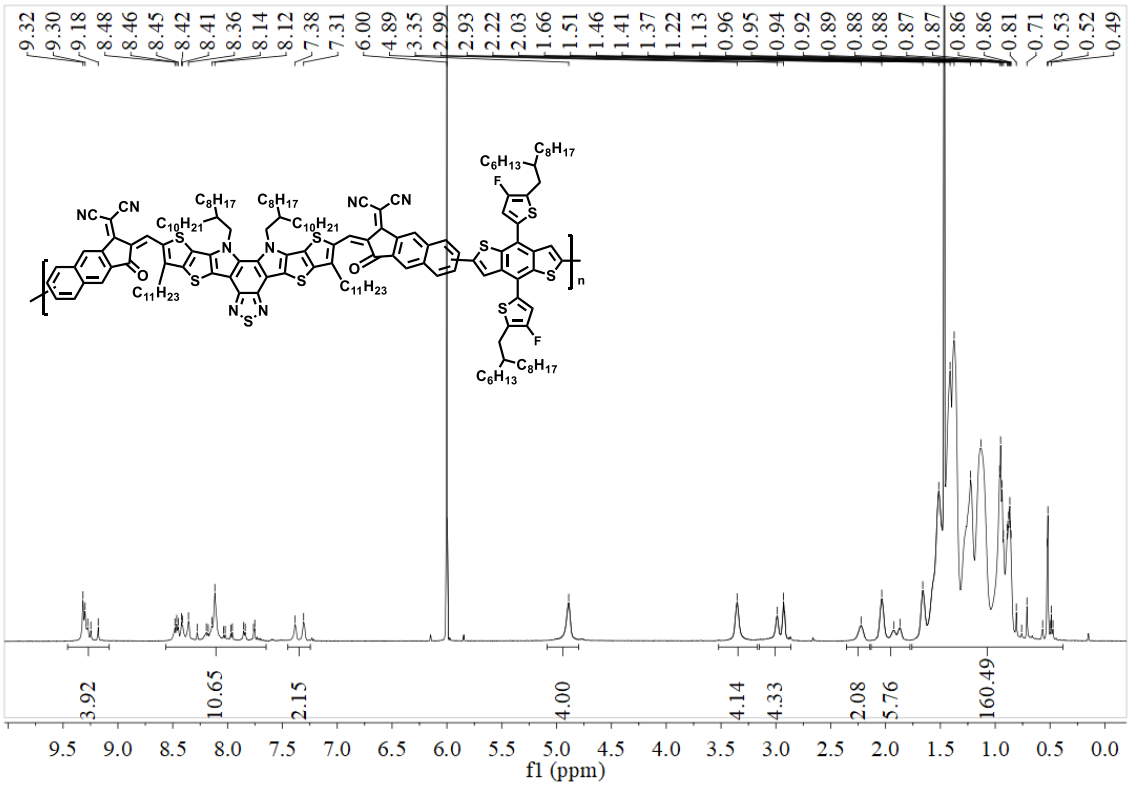

Figure S20. ^{1}H NMR of PYN-BDTF in $C_2D_2Cl_4$.

9. References

(1) Kato, D.; Sakai, H.; Tkachenko, N. V.; Hasobe, T., High-Yield Excited Triplet States in Pentacene Self-Assembled Monolayers on Gold Nanoparticles through Singlet Exciton Fission. *Angew. Chem.* **2016,** *55*, 5230-5234.

(2) Zhu, W.; Spencer, A. P.; Mukherjee, S.; Alzola, J. M.; Sangwan, V. K.; Amsterdam, S. H.; Swick, S. M.; Jones, L. O.; Heiber, M. C.; Herzing, A. A.; Li, G.; Stern, C. L.; DeLongchamp, D. M.; Kohlstedt, K. L.; Hersam, M. C.; Schatz, G. C.; Wasielewski, M. R.; Chen, L. X.; Facchetti, A.; Marks, T. J. Crystallography, Morphology, Electronic Structure, and Transport in Non-Fullerene/Non-Indacenodithienothiophene Polymer:Y6 Solar Cells. *J. Am. Chem. Soc.* **2020,** *142*, 14532-14547.